Primary and Secondary Effects of K^+-channels Block During Atrial Fibrillation and its Rate Dependency

Fazeelat Mazhar[1], Chiara Bartolucci[1], Stefano Severi[1]

[1]Univeristy of Bologna, Cesena, Italy

Abstract

Selective inhibition of atrial fibrillation (AF) can be of therapeutic benefit for reducing the AF burden. The concept of atrial-selective block of K^+ channels mainly ultra-rapidly activating and delayed-rectifier (I_{Kur}) and transient outward (It_o) current may suppress AF without the risk of ventricular proarrhythmic effects. K^+-channels block alters electrophysiology through a combination of primary and secondary effects. In addition, the underlying mechanisms behind the rate dependent response of such blockers both under sinus rhythm (SR) and AF condition is not yet fully clear.

In this work, we have dissociated the primary and secondary response of low dose concentration of K^+-channel block (4-AP and AVE0118) on human atrial electrophysiology by clamping one current at a time. As a result, under SR condition, 4-AP abbreviates the AP duration (APD) and that was because of the secondary rise of the I_{Kr} current. In contrast, during AF, the lengthening of APD in response to 4-AP was because of AP mediated rise in I_{CaL} current. At higher rates, in SR but not in AF condition, both drugs perturb the rate dependent shortening of APD and slows the AP upstroke velocity at higher rates because of unavailability of Na^+ channels. Our analysis suggest that K^+-channel block can AF induced burden.

1. Introduction

The principal approach for suppressing the occurrence of atrial fibrillation (AF) is the application of antiarrhythmic drug therapy. I_{Kur} current is considered an atrial-selective target for antiarrhythmic drugs with a favourable benefit-to-harm relation. Since it contributes only to atrial repolarization with no effect on ventricular action potential (AP) [1]. The anticipated effect of blocking an outward current on the AP is a lengthening of the duration (APD). However, in human atrial trabeculae, I_{Kur} channel blockage abbreviates the APD under SR and prolongs it under AF condition [2]. In addition, blocking multiple K^+ channels (I_{Kur} and I_{to} currents) in a dog atria was found to prolong the effective refractory period (ERP) under both SR and AF conditions with no chance of inducing ventricular arrhythmias (like long QT syndrome) [3]. Similarly, under AF the K^+-channels block response is always lengthening of AP and the ERP even for higher rates that might be favourable in reversing the AF induced burden [4].

The underlying mechanism is debatable since at basal rate, in some studies it is either related to secondary rise in I_{Kr} current [2], or to a secondary block of I_{Na} current [5], or even to a secondary enhancement of I_{NaCa} reverse mode [6]. To understand the mechanisms more in depth, in this work we aim to dissociate the primary and secondary effects of K^+-channels block on electrophysiology. For this, we have used the power of computational modelling that provides an efficient way to investigate the useful insights under physiological and pathological conditions. We have clamped one current at a time to dissect the primary and secondary mechanisms under SR and AF conditions. In addition, we have extended our analysis for higher AF relevant rates, to evaluate the extent by which K^+ channel block can be useful in reversing the AF induced burden.

2. Methods

2.1 Model updates

In this work we have utilized our electro-mechanical model for human atrial CMs [7] namely MBS2023 (*Mazhar-Bartolucci-Severi 2023*), with few proposed updates. Despite the model provides a physiological Ca^{2+}-transient (CaT) followed by a physiological twitch, one of the limitations highlighted in the model was the slow relaxation in the later phase of decay. The slow uptake kinetics of the sarcoplasmic reticulum (SR) makes the Ca^{+2} transient decay slower, eventually slowing the twitch relaxation.

In MBS2023, the cross bridge (XB) transition rates were adopted from RDQ contraction model [8]. However, in RDQ, the XB cycling was quite fast in comparison to what is observed in experiments [9]. In addition, the thin filament regulatory unit (RU) rates were comparatively slow. Therefore, the contraction model transition rates were retuned and are listed in Table 1. The re-tuning of

contractile parameters resulted into acceleration of Ca^{2+}-handling machinery. Consequently, the RyR_{ss} inactivation gate time constant was made faster from 60 to 30msec as shown in Table 1. In addition, $RyR_{ss,adapt}$ maximum and minimum levels were restored as was in Koivumäki 2011 model [10]

Few ionic currents were also updated like, the slope of I_{Kr} inactivation was halved, in this way the current was completely inactivated at positive potentials. The inactivation time formulation for I_{Kr} was based on rabbit experimental data in the parent model [11] therefore, it was adapted from Courtemanche 1998 model [12] that was based on human data [13]. Other than this, in the parent model, I_{to} formulation was based on rabbit experimental data therefore, it was updated with respect to the experimental data [13]. To compensate the increased Ca^{2+} in the cytoplasm, the inward mode of I_{NaCa} current was enhanced by increasing f_{CaNCX} from 1 to 1.3. Apart from this few current conductances were updated and are listed in Table 1.

Table 1: List of parameters updated in MBS2023 model.

	Parameter		MBS2023	Updates
Contraction	γ	(-)	12	5
	K_{off}	(s^{-1})	100	130
	K_{basic}	(s^{-1})	12	40
	r_{0P}	(s^{-1})	134.31	35
Electrophysiology	$RyR_{ss\ inact}$	(s)	60	23
	g_{to}	(nS)	8.175	12.26
	g_{Na}	(nS)	350	250
	g_{Kr}	(nS)	0.5	2
	g_{Ks}	(nS)	1	2

2.2 Simulation setup

Using the control updated version of MBS2023, we incorporated the AF induced remodelling effect as was done in our previous work [14]. Following the incremental approach, we included the effect of Ca^{2+}-buffering, troponin (TRPN) in specific, by reducing its expression and TRPN-Ca^{2+} binding affinity by 25% and 20% respectively [15].

Using control/SR and AF versions of updated MBS2023 model, we analysed the response of K^+ channels block using I_{Kur} specific 4-AP (5μM) and non-specific AVE0118 blockers (6μM) at basal rate 1Hz and extended it for a range of BCLs [2 1 0.5 0.33 0.25] sec. The equivalent percentage of currents block using 4-AP was 35% block of I_{Kur} and with AVE0118 was 68% I_{Kur} and 29% I_{to} block. To differentiate well among the primary and secondary effects of K^+-channel block, we have run the simulation with drug applied condition while clamping one current to its basal state i.e. without drug condition. We have clamped I_{CaL} and I_{Kr} currents and repeated the simulations for each current at a time. Biomarkers that were measured for the analysis were AP duration at 90% of repolarization (APD_{90}), maximal upstroke velocity (dV/dt_{max}).

3. Results

At basal rate 1Hz, the AP waveform for SR and AF conditions is shown in Figure 1. The updated MBS2023 model under SR, has elicited an AP that is less triangular now and closer to spike and dome morphology (in blue). Under SR condition, 4-AP (in red) abbreviated the APD and AVE0118 (in yellow) lengthened it. In addition, both drugs elevated the plateau potential of the AP resulting in enhanced Ca^{2+} entry via I_{CaL} current (middle left panel). Meanwhile, the enhanced Ca^{2+}dependent inactivation (CDI) has reduced the peak I_{CaL} current while an AP mediated rise in plateau phase can be seen. This behaviour was more appreciated in case of AVE0118 drug. The elevation in AP plateau potential has given a secondary rise in I_{Kr} current (lower left panel).

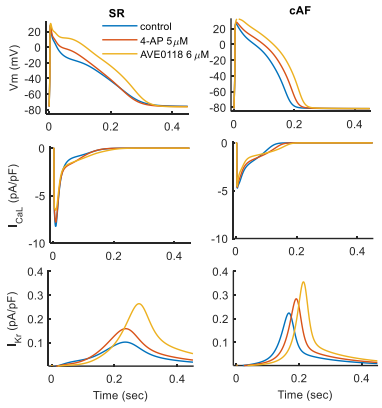

Figure 1: Updated MBS2023 model (in blue) action potential (AP) (top panel), I_{CaL} (middle panel), and I_{Kr} (bottom panel) response upon applying 5μM 4-AP (in red), 6μM AVE0118 (in yellow) under SR (on left) and cAF (on right) conditions at 1Hz basal rate.

Under AF condition, both drugs lengthen the AP with enhanced plateau level (top right panel). AF-remodeled I_{CaL} current demonstrates a biphasic response in presence of the drug i.e. a reduction in lower plateau followed by an increase. On the other hand, drug associated secondary rise of I_{Kr} current was even more pronounced in AF condition.

To understand the underlying mechanisms, we have simulated both drug response under I_{CaL} and I_{Kr} clamp condition as shown in Figure 2.

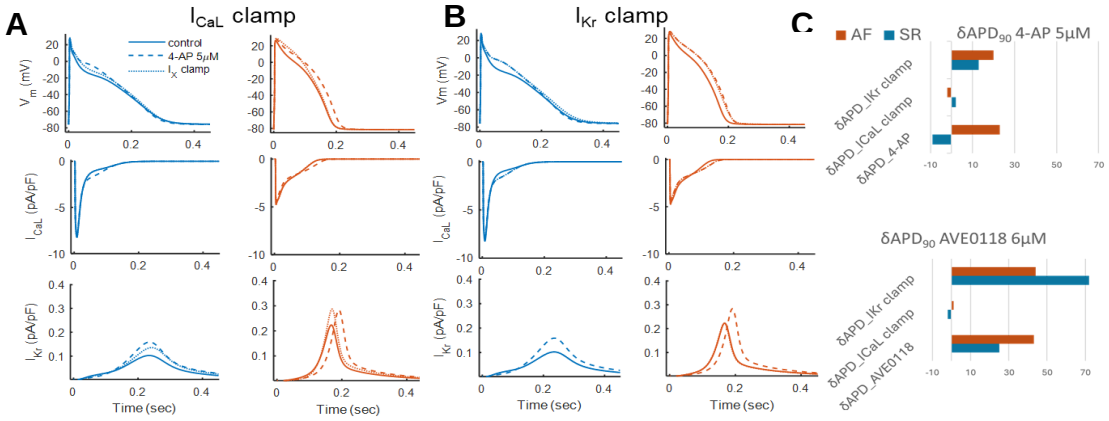

Figure 2: 4-AP and AVE0118 drug response on updated MBS2023 model (dashed line) under one current clamped condition for both SR (in blue) and AF (in red) conditions. Currents clamped (in dotted line) are I_{CaL} (A) and I_{Kr} (B) with biomarker (C) change in action potential duration $\delta APD = APD_{drug} - APD_{control}$.

Under SR condition, the change in AP duration at 90% of repolarization APD ($\delta APD = APD_{drug} - APD_{control}$) (Figure 2C in blue bars) was negative under 4-AP that converted into large positive value under I_{Kr} clamped condition. Therefore, AP mediated secondary rise in I_{Kr} (Figure 2B lower panel) was the main underlying mechanism behind the APD shortening under SR condition using 4-AP. Furthermore, under AF condition, clamping I_{Kr} current did not make much difference on the AP shape (Figure 2B top right panel). Interestingly, elevation of I_{CaL} in the late inactivation phase (Figure 2A middle right panel) was the main driving mechanism behind the AP lengthening under AF since on clamping I_{CaL}, δAPD was converted into a negative quantity hence a shortening effect. The same set of simulations were repeated for AVE0118, where it was found that under both SR and AF conditions, clamping of I_{CaL} converted the δAPD from positive to a negative quantity where I_{Kr} clamp was less important.

The drugs were applied to the model for higher rates under SR and AF conditions as shown in Figure 3. Using 4-AP, under SR condition, the APD shortening was converted into lengthening for shorter BCLs (0.33, 0.25sec) (Figure 3A) and APD was always lengthening under AF condition (Figure 3B) as is seen in the experiments [5] as quantified by δAPD in Figure 3C. For higher rates, for instance BCL 0.33, 0.25 sec, the AP was incomplete, and this was clearer for AVE0118 trace (in dotted line). Apart from this, the excitation was slowed down by K^+-channel blockers, at BCLs from 330msec to onwards as quantified by the change in maximal upstroke velocity ($\delta dV/dt_{max}$) behavior (Figure 3C bottom). Under cAF condition, the rate dependent APD shortening effect was preserved however shifted to lower values and the excitation was least effected. The excitation of the AP was enhanced under cAF condition but remained unaffected by the drug exposure (Figure 3C).

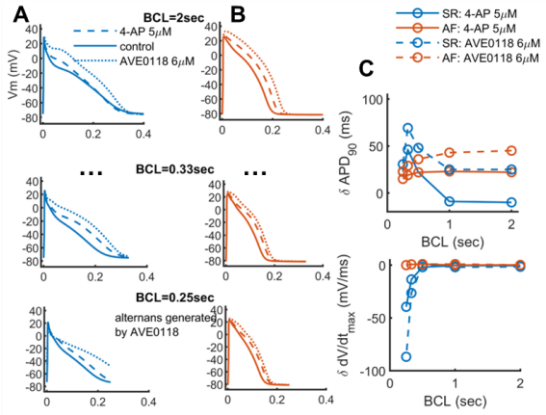

Figure 3: K^+-channel block effect on action potential for varying BCL [2 … 0.33 0.25]sec under SR (in blue) and AF (in red) conditions. The AP biomarkers were quantified as change in value with respect to the drug applied like δAPD and $\delta dV/dt_{max}$.

The therapeutic potential of K^+-channel blockers was analysed on the AP characteristics under SR and AF conditions. For this, the afterdepolarization abnormalities like EADs were induced by the sensitization of RyR_{ss} in the model as shown in Figure 4. For AF condition, EADs were obtained only by reversing some remodelling effects as shown in Figure 4 legend. When applied 4-AP, the elevated plateau potential rescues the slow voltage dependent inactivation (VDI) of I_{CaL} current (lower panel).

4. Discussion and Conclusion

The current work provides a framework to analyze the extent by which K^+-channel block can be effective in reducing AF burden. Moreover, we have highlighted the underlying mechanisms for K+-channel block for a range of varying BCLs.

At basal rate, 4-AP shortened the APD in SR and

lengthened under AF. The secondary rise of CaT in the ss strengthens the CDI effect however it remains submissive in the presence of elevated plateau of the AP thereby activating more I_{CaL} current. The preserved I_{Kur} integral under 4-AP can be speculated as a secondary effect of I_{Kur} block. The enhanced plateau creates positive feedback on I_{Kur} current by slowing the inactivation phase. Hence, the increase of I_{CaL} inward current at lower rates in SR is compensated by the slow inactivation of I_{Kur} outward current and this get reversed at higher rates. At higher rates, in SR condtion, 4-AP reduced the excitation that was because of depolarization of V_{rest} because of incomplete AP as was also observed in experiments [5]. Overall, this analysis can be extended to compare the efficacy of specific and non-specific I_{Kur} blockers towards other AF related abnormalities like type 3-EADs and DADs.

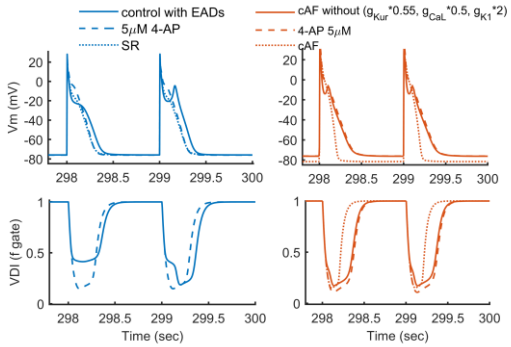

Figure 4: K+-channel block effect on early afterdepolarizations (EADs) under SR (on left) and AF (on right) conditions.

Acknowledgments

C.B. and S.S. have received funding from the European Union – Next Generation EU through the Italian Ministry of University and Research under PNRR - M4C2- I1.3 Project PR 00000019 "HEAL ITALIA" to S.S. CUP J33C22002920006.

S.S. has received funding from European Union-SMASH-HCM project under grant agreement number 101137115.

References

[1] U. Ravens and E. Wettwer, "Ultra-rapid delayed rectifier channels: molecular basis and therapeutic implications," *Cardiovasc. Res.*, vol. 89, no. 4. pp. 776–785, 2011.

[2] E. Wettwer *et al.*, "Role of I_{Kur} in controlling AP shape and contractility in the human atrium: Influence of cAF," *Circulation*, vol. 110, no. 16, pp. 2299–2306, 2004.

[3] A. Burashnikov *et al.*, "Atrial-selective prolongation of refractory period with AVE0118 is due principally to inhibition of Na^+ channel activity," *J Cardiovasc Pharmacol*, vol. 59, no. 6, pp. 539–546, 2012.

[4] U. Schotten *et al.*, "Blockade of atrial-specific K^+-currents increases atrial but not ventricular contractility by enhancing reverse mode Na^+/Ca^{2+}-exchange," *Cardiovasc Res*, vol. 73, no. 1, pp. 37–47, 2007.

[5] J. Ford *et al.*, "The positive frequency-dependent electrophysiological effects of the I_{Kur} inhibitor XEN-D0103 are desirable for the treatment of AF," *Heart Rhythm*, vol. 13, no. 2, pp. 555–564, 2016.

[6] F. Mazhar *et al.*, "A detailed mathematical model of the human atrial cardiomyocyte: integration of electrophysiology and cardiomechanics Key points," *J Physiol*, pp. 1–41, 2023.

[7] F. Regazzoni *et al.*, "Biophysically detailed mathematical models of multiscale cardiac active mechanics," *PLoS Comput Biol*, vol. 16, no. 10, 2020.

[8] N. Piroddi *et al.*, "Tension generation and relaxation in single myofibrils from human atrial and ventricular myocardium," *Pflugers Arch*, vol. 454, no. 1, pp. 63–73, 2007.

[9] J. T. Koivumäki *et al.*, "Impact of SR calcium release on calcium dynamics and AP morphology in human atrial myocytes: A computational study," *PLoS Comput Biol*, vol. 7, no. 1, 2011.

[10] A. Nygren *et al.*, "Mathematical model of an adult human atrial cell the role of K Currents in repolarization," pp. 63-81, 1998.

[11] M. Courtemanche *et al.*, "Ionic mechanisms underlying human atrial AP properties: insights from a mathematical mode," 1998.

[12] Z. Wang *et al.*, "Delayed rectifier outward current and repolarization in human atrial myocytes, 1993.

[13] Z. Gao *et al.*, "Effects of diltiazem and nifedipine on transient outward and ultra-rapid delayed rectifier K^+ currents in human atrial myocytes," *Br J Pharmacol*, vol. 144, no. 4, pp. 595–604, 2005.

[14] F. Mazhar *et al.*, "Investigation of key cellular targets in AF induced electromechanical remodeling using human atrial cardiomyocytes model," in *CinC*, IEEE Computer Society, 2023.

[15] Fakuade *et al.*, "Impaired Intracellular calcium buffering contributes to the arrhythmogenic substrate in atrial myocytes from patients with atrial fibrillation," *Circulation*, vol. 150, pp. 544-559, 2024.

Address for correspondence:
Stefano Severi
Via Cesare Pavese, 50, 47521 Cesena FC, Italy
stefano.severi@unibo.it